



**HAL**  
open science

## Eastern Tropical Atlantic Mixed Layer Depth: Assessment of Methods from In Situ Profiles in the Gulf of Guinea from Coastal to High Sea

Benjamin Kouadio N'Guessan, Aka Marcel Kouassi, Albert Trokourey, Elisee Toualy, Desire Kouame Kanga, Patrice Brehmer

► **To cite this version:**

Benjamin Kouadio N'Guessan, Aka Marcel Kouassi, Albert Trokourey, Elisee Toualy, Desire Kouame Kanga, et al.. Eastern Tropical Atlantic Mixed Layer Depth: Assessment of Methods from In Situ Profiles in the Gulf of Guinea from Coastal to High Sea. *Thalassas: An International Journal of Marine Sciences*, 2019, 36 (1), pp.201-212. 10.1007/s41208-019-00179-7 . hal-02873902

**HAL Id: hal-02873902**

**<https://hal.science/hal-02873902>**

Submitted on 5 Jul 2023

**HAL** is a multi-disciplinary open access archive for the deposit and dissemination of scientific research documents, whether they are published or not. The documents may come from teaching and research institutions in France or abroad, or from public or private research centers.

L'archive ouverte pluridisciplinaire **HAL**, est destinée au dépôt et à la diffusion de documents scientifiques de niveau recherche, publiés ou non, émanant des établissements d'enseignement et de recherche français ou étrangers, des laboratoires publics ou privés.

---

## Eastern Tropical Atlantic Mixed Layer Depth: Assessment of Methods from In Situ Profiles in the Gulf of Guinea from Coastal to High Sea

N'Guessan Benjamin Kouadio <sup>1,2,\*</sup>, Kouassi Aka Marcel <sup>1</sup>, Trokourey Albert <sup>2</sup>, Toualy Elisée <sup>3</sup>, Kanga Desiré Kouamé <sup>1,2</sup>, Brehmer Patrice <sup>4</sup>

<sup>1</sup> Centre de Recherches Océanologiques (CRO), Abidjan, Côte d'Ivoire

<sup>2</sup> UFR SSMT, Université Felix Houphouët-Boigny, Laboratoire de Chimie-Physique, Abidjan, Côte d'Ivoire

<sup>3</sup> UFR SSMT, Université Felix Houphouët-Boigny, Laboratoire de Physique de l'Atmosphère et de Mécanique des Fluides (LAPA-MF), Abidjan, Côte d'Ivoire

<sup>4</sup> IRD, Univ Brest, CNRS, Ifremer, Lemar, Délégation Régionale IRD Oues, tPlouzané, France

\* Corresponding author : Benjamin Kouadio N'Guessan, email address :

[nguessan.k.benjamin@gmail.com](mailto:nguessan.k.benjamin@gmail.com)

---

### Abstract :

To assess the eastern Atlantic tropical mixed layer depth (MLD) at 4°W in the Gulf of Guinea, water temperature and density profiles from over five hundred historical observational Conductivity – Temperature – Depth (CTD) data were used. These data, obtained from key oceanographic survey databases covering 60 years (1956 to 2016) were used for a numerical and visual determination of the MLD. The numerical approach consists of the use of the algorithms of three methods; while the visual estimation of the MLD were made on both temperature and density profiles. The numerical approaches were evaluated by comparing their results on the determination of tropical MLD with those of the visual inspections by means of statistical and graphical analysis in order to determine the most suitable method for the determination of MLD in the study area. Our results show that the Boyer Montegut density threshold method (potential density) with the constant criterion  $\Delta\sigma = 0.03 \text{ kg.m}^{-3}$  and a reference depth of ten meters is the most appropriate for determining the MLD in the Gulf of Guinea regardless the season. However, in the situation where only temperature profiles are available it is advisable to estimate MLD using the Lorbacher curvative method.

**Keywords :** Mixed layer depth, Gulf of Guinea, Atlantic Ocean, Density, Temperature

36           **1. INTRODUCTION**

37    The mixed layer depth (MLD) of the ocean is commonly considered as the area near the surface  
38    with vertically quasi-uniform ocean tracers (temperature, salinity, density) above a layer of  
39    more rapid vertical changes (**Lorbacher et al., 2006**). It is the manifestation of vigorous  
40    turbulent mixing processes which are active in the upper layers of the ocean. The transfer of  
41    mass, momentum and energy across the mixed layer provides the source of almost all ocean  
42    motions and the thickness of the mixed layer determines the heat content of the mechanical  
43    inertia of the layer that directly interact with the atmosphere (**de Boyer Montégut et al., 2004**).

44    The MLD is generally estimated from temperature and density profiles using several  
45    approaches. The first two methods are the threshold and gradient approaches (**Sprintall and**  
46    **Tomczak 1992; Sprintall and Roemmich 1999; Kara et al., 2000; Thomson and Fine,**  
47    **2010**). The threshold and gradient methods fix the shallowest depth where chosen threshold or  
48    gradient criterion is achieved. The third method was developed by **Lorbacher et al. (2006)** who  
49    estimated MLD using the curvative of the profile. This approach searches for the first extreme  
50    curvative of the profile, analyses the profile at nearby levels and defines MLD. The fourth  
51    method was that of **Holte and Talley (2009)** which is a hybrid method for finding the mixed  
52    layer depth (MLD) of individual ocean profiles (temperature, salinity, and density). This  
53    approach selects the final MLD from possible MLD values estimated from the threshold and  
54    gradient methods but also by looking for some physical characteristics of the profile such as  
55    thermocline / pycnocline, location of maxima or minima of the profile, intrusions to the base of  
56    the mixed layer.

57    The Gulf of Guinea is a dynamic and complex ecosystem along the equatorial West African  
58    coasts, approximately extending from Guinea–Bissau to Gabon (**Tilot and King 1993, Binet**  
59    **and Marchal 1993; Nieto et al., 2017**). This region benefits from a high level of incoming  
60    solar radiation and hot waters that promotes plankton which in turn supply food for fishes and  
61    sustain fisheries, a key source of revenue for economic and social development for the countries  
62    of the region (**Nieto et al., 2017**). The Gulf of Guinea is a very important area for fisheries  
63    showing a high degree of both physical and biological environmental variability (**Hardman-**  
64    **Mountford, 2000**) whose study is facing lack of observational data of good quality and spatio-  
65    temporal resolution.

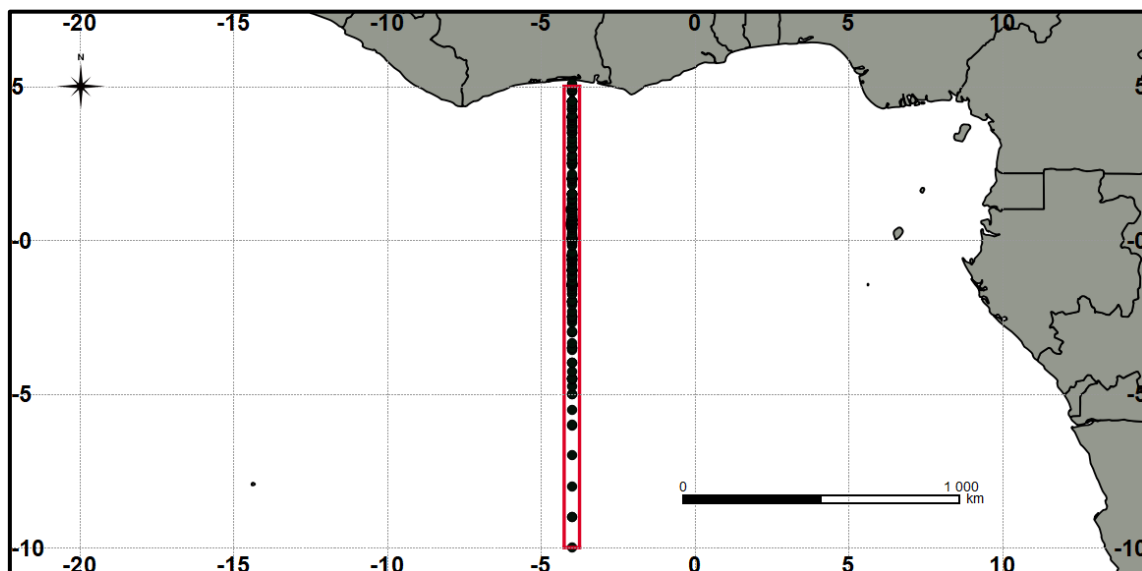
66 Studies in relation with mixed layer in the Gulf of Guinea were undertaken by **Peter et al.**  
67 **(2006)** and **Wade (2010)** respectively on salt and heat balance of the mixed layer from a set of  
68 satellite and observation data. The threshold method was used by these two studies.

69 The objective of this study is to explore several approaches commonly used to calculate the  
70 MLD and to determine the most suitable for its determination in the Gulf of Guinea.

## 71 1. METHODS

### 72 1.1. Data, processing and control

73 The data used in this study were extracted from a box centered on  $4^{\circ}\text{W} \pm 0.25^{\circ}$  and limited by  
74 latitudes  $5^{\circ}\text{N}$ - $10^{\circ}\text{S}$  (Fig. 1).



75 **Fig. 1** Study area showing the red box ( $5^{\circ}\text{N}$ ,  $4.25^{\circ}\text{W}$ ;  $5^{\circ}\text{N}$ ,  $3.75^{\circ}\text{W}$ ;  $10^{\circ}\text{S}$ ,  $4.25^{\circ}\text{W}$ ;  $10^{\circ}\text{S}$ ,  $3.75^{\circ}\text{W}$ ) where  
76 data were extracted at  $4^{\circ}\text{W}$  in the Gulf of Guinea  
77

78 These are historical observational CTD (Conductivity-Temperature-Density) data of irregular  
79 spatial and temporal resolution from three oceanographic survey databases: The Systèmes  
80 d'Informations Scientifiques pour la Mer (SISMER) data (<https://data.ifremer.fr/SISMER>)  
81 from 1956 to 2016, the World Ocean Database 2013 (WOD13) data (**Boyer et al., 2013**)  
82 extracted between 1971 and 2016 and the CORIOLIS data (<http://www.coriolis.eu.org>)  
83 covering the period 1956 to 2016. The number of some stations from SISMER were reassigned  
84 to avoid duplicates.

85 Stations without temperature, salinity or pressures (depths) data were not considered. The data  
86 files were then restructured by year and by campaign. The potential densities were calculated

87 and the depths (in meters) of the WOD13 data profiles were converted to pressures (dbar) using  
88 the CSIRO SeaWater Library (version 3.3.1) in Matlab software (Matrix Laboratory).

89 The temperature, salinity and density profiles from the raw data of the stations were plotted.  
90 Visual inspection and correction of these profiles were also performed according to  
91 **Maheswaran (2004)** and **Nahavandian (2014)**. Profiles containing no more than three depth  
92 levels points were not considered because the algorithm computes moving averages of order 3.  
93 Profiles with low vertical resolutions ( $>10$  m) in the first 50 meters were removed. Finally,  
94 profiles with a maximum depth of less than or equal to 50 m were also deleted because,  
95 according to the Climatology of **de Boyer Montégut et al. (2004)**, the study area has a MLD  
96 maximum around 60 m. For CTD profiles with one or more missing values in the first 100  
97 meters, the values were replaced by the bottle data from the same station and same campaign if  
98 they are available. When no replacement value existed for intermediate levels between two  
99 measured values, they were replaced by the average of the two values that surround it.

100 From these data treatments, 1209 stations were obtained: 417 for WOD13, 122 for CORIOLIS  
101 and 670 for SISMER databases. The Individual temperature, salinity, and density profiles of  
102 these stations were used for numerical determination of MLD using the algorithms of **Holte**  
103 **and Talley (2009)**, **Thomson and Fine (2003)** and **Lorbacher et al. (2006)**. Data that did not  
104 satisfy the inclusion conditions of the algorithms were removed. Finally, a total of 516 stations  
105 spanning 46 years between 1971 and 2016 are obtained and displayed in Table 1.

106

**Table 1:** Number of stations (N = 516) per year and month between 1971 and 2016 used for the study.

Years	Hot season								Cold season				Total
	Nov.	Dec.	Jan.	Feb.	Mar.	Apr.	May.	Jun.	Jul.	Aug.	Sep.	Oct.	
1971	4	-	-	-	-	-	-	-	-	-	-	-	4
1972	-	-	-	-	-	-	1	-	-	-	18	-	19
1973	11	-	-	-	-	-	-	-	-	-	-	-	11
1974	-	-	-	-	-	-	-	-	13	-	-	-	13
1975	-	-	3	-	-	-	-	-	-	-	-	-	3
1977	-	-	22	7	-	-	-	-	6	-	-	-	35
1978	-	-	-	-	-	-	-	-	-	129	24	-	153
1979	-	-	19	-	-	-	-	7	-	-	-	-	26
1980	-	-	1	-	-	-	-	-	-	-	-	-	1
1982	11	-	-	-	-	-	-	-	12	-	-	-	23
1983	8	-	-	8	-	13	-	-	-	11	-	1	41
1984	-	-	-	12	-	-	25	14	22	-	-	-	73
1985	-	-	-	-	-	-	-	-	7	-	-	-	7
1988	-	-	-	-	15	-	-	-	-	-	-	-	15
1993	-	-	1	-	23	-	-	-	-	-	-	-	24
2004	-	-	-	-	1	-	-	-	-	-	-	-	1
2005	-	-	-	-	-	-	-	-	-	-	-	1	1
2006	-	-	-	-	-	1	1	-	-	-	-	-	2
2007	1	1	-	-	-	-	-	-	-	-	-	-	2
2008	-	-	-	2	1	-	-	-	-	2	-	-	5
2009	-	-	-	-	-	-	-	-	1	-	-	1	2
2010	-	-	-	-	-	-	-	-	1	-	-	-	1
2011	-	-	1	-	-	-	-	-	1	-	2	-	4
2012	-	-	-	-	-	1	-	1	-	1	-	1	4
2013	-	-	1	-	-	1	-	-	-	-	-	-	2
2014	-	1	-	-	-	-	20	2	-	1	-	-	24
2015	1	-	2	-	1	-	-	-	-	-	2	1	7
2016	-	3	-	1	-	-	5	2	-	1	1	-	13
<b>Total</b>	<b>36</b>	<b>5</b>	<b>50</b>	<b>30</b>	<b>41</b>	<b>16</b>	<b>52</b>	<b>26</b>	<b>63</b>	<b>145</b>	<b>47</b>	<b>5</b>	<b>516</b>

107 **1.2. Numerical and visual determination of MLD**

108 The temperature and density profiles were first vertically interpolated before the determination  
109 of the MLD. The numerical determination of MLD were based on the algorithms of three  
110 methods developed by **Lorbacher et al., (2006), Thomson and Fine (2003) and Holte and**  
111 **Talley (2009)**. The Holte and Talley method uses the threshold and gradient approaches and  
112 special algorithms for either temperature or density to estimate MLD. The visual determinations  
113 were made by visual inspection of the MLD on the temperature and density profiles of the 516  
114 stations graphically represented. The algorithms and their results were abbreviated respectively  
115 by LORB, TF and HT (Table 2).

**Table 2:** Codification of mixed layer depth (MLD) obtained from different methods of determination, based on conductivity temperature and depth (CTD) profile. LORB: Lorbacher method; TF: Thomson and Fine method; HT: Holte and Talley method. Temp: MLD from temperature profile. Dens: MLD from density profile. Temp Thres: Temperature threshold criterium; Dens Thres: Density threshold criterium; Dens Grad: Density Gradient criterium; Algo: MLD from temperature or density algorithm. Visu: MLD from visual inspection. The alphabetic letters represent these different methods variants.

Methods	Codification of results (MLD)	
	Temperature-based MLD	Density-based MLD
<b>Holte and Talley, 2009</b> (HT)	A: HT Temp Algo C: HT Temp Thres E: HT Temp Grad	B: HT Dens Algo D: HT Dens Thres F: HT Dens Grad
<b>Lorbacher et al., 2006</b> (LORB)	G: LORB Temp	H: LORB Dens
<b>Thomson and Fine, 2003</b> (TF)	I: TF Temp	J: TF Dens
<b>Visual inspection</b>	Visu Temp	Visu Dens

### 1.3. Numerical methods evaluation

The evaluation of the methods consisted of comparing the results (MLD) of the different variants of the three numerical methods with visually determined MLD (which serve as reference values) on the temperature and density profiles in both hot and cold seasons (You, 1995, Sprintall and Roemmich, 1999, Kara et al., 2000, Ohno et al., 2009). This is done through statistical and graphical analysis of method performance from Taylor diagrams (Taylor, 2001) and 2D diagrams of linear correlations between pairs of methods (Maheswaran, 2004; Nahavandian, 2014).

#### 1.3.1. Evaluation using the Taylor diagrams

Two diagrams are drawn: One for temperature-based methods and another one for density-based methods. Ten variants represented by alphabetical letters are evaluated: A, C, E, G and I for the five variables based on temperature; B, D, F, H and J for the five density based. The reference values are represented by Visu Temp and Visu Dens. Three different statistics are analyzed: mean, standard deviation (STD), Root-Mean-Square Deviation (RMSD) and the correlation coefficient of Bravais-Pearson ( $r$  instead of  $R^2$ ). The lower the RMSD, the closer the variant is to the reference and is therefore able to reproduce the reference values (Taylor, 2001).

#### 1.3.2. Evaluation using the linear correlation diagrams

Linear correlation diagrams were used to determine the adjustment line, the linear correlation coefficient ( $R^2$ ) test the significance of the correlation and analyze the distribution of the scatter plot with respect to the first bisector, which gave information on the bias of methods.

137 The significance of the correlations was tested through the values of the *p-values* (Alboukadel,  
 138 2018). These diagrams compare digital MLD and visual MLD. The evaluation target for the  
 139 numerical variant whose linear correlation with the visual methods has the highest correlation  
 140 coefficient R and whose results are the least biased possible.

141 Finally, the numerical variant chosen to determine the MLD is the one that has the following  
 142 characteristics: The point representing the variant is the closest to that of the reference on the  
 143 Taylor diagram; This variant has a high correlation coefficient with the reference; It gives the  
 144 most comparable results possible with the reference, that is to say does not underestimate nor  
 145 overestimate the MLD compared to the reference values on the 2D diagrams.

## 146 2. RESULTS AND DISCUSSIONS

### 147 2.1. Analysis of MLD numerical determinations

148 Five hundred and sixteen (516) MLD values including 260 for the cold season and 256 for the  
 149 hot season are determined. Table 3 displays the minimum, maximum and average values of  
 150 MLD.

**Table 3:** MLD results statistics based on numerical methods. For abbreviations refer to Table 2.

	Statistics	HT Temp Algo	HT Dens Algo	HT Temp Thres	HT Dens Thres	HT Temp Grad	HT Dens Grad	LORB Temp	LORB Dens	TF Temp	TF Dens
Hot season	Minimum	10,50	10,00	10,50	10,00	11,00	11,00	1,99	0,00	10,19	10,15
	Maximum	52,00	53,00	52,50	52,00	51,00	45,00	49,70	49,67	52,18	46,34
	Mean	24,99	22,36	23,66	19,12	17,71	13,43	19,51	13,16	25,21	21,86
Cold season	Minimum	10,00	10,00	10,00	10,00	11,00	11,00	3,60	0,00	10,09	10,13
	Maximum	63,00	45,00	62,00	46,00	57,00	33,00	61,94	46,28	72,39	43,56
	Mean	21,86	20,46	20,79	18,90	16,53	13,30	18,24	14,38	21,23	19,62

151 The MLD estimated by the HT, TF and LORB numerical methods are between 0 and 72 m. In  
 152 both hot and cold seasons, the minimum values obtained from HT and TF methods are all  
 153 around 10 m (reference depth). The maximum MLD is obtained from the temperature profiles  
 154 with the TF method and the lowest MLD with LORB methods regardless the season.

155 The LORB method, unlike the threshold and gradient methods, does not critically depend on  
 156 the choice of the reference depth. According to Lorbacher et al. (2009), the curvative method  
 157 generally gives lower MLD than with the temperature threshold criterion of de Boyer  
 158 Montégut et al. (2004). The results of their work showed that in about 70% of the high-  
 159 resolution CTD profiles that were the subject of their work, their method underestimated the

160 values with respect to de Boyer Montégut temperature threshold criterion (**de Boyer Montégut**  
 161 **et al., 2004**). The low observed values could also be explained by the interpolations (linear  
 162 and/or exponential) between the different depths leading to underestimation of the MLD.  
 163 Moreover, in the tropics, at about  $\pm 20^\circ$  latitude of the equator, the water column is weakly  
 164 stratified below the surface and the temperature profiles in the upper part of the main  
 165 thermocline are concave, producing vertical gradients that sometimes result in lower MLD  
 166 (**Lorbacher et al., 2009**). Finally, according to **Tanguy et al. (2010)**, the Lorbacher method is  
 167 based on gradient calculations and is very sensitive to small variations that may be caused by  
 168 diurnal mixing or may be influenced by a weaker stratification at the bottom of the mixed layer.

169 Table 4 shows the proportions (%) of MLD determined with the different possibilities in the  
 170 HT method.

**Table 4:** Proportions (in %) of mixed layer depth (MLD) determined with the different HT method possibilities.

	Threshold criterion	Gradient criterion	Intersection between thermocline fit line (pycnocline) and the line fitted to the profile « adjustment lines criterion »	Other possibilities
Temperature profiles	54	8	35	3
Density profiles	37	11	49	3

171 The HT method has six variants that use in addition to threshold and gradient criteria, the  
 172 process of assigning the MLD by the algorithm itself. This process chooses among several  
 173 possibilities of values of MLD, the value which is appropriate for the type of studied profile.

174 Table 4 shows that 35% of the MLD correspond to the « adjustment lines criterion »; 8% of the  
 175 MLD are obtained from the gradients criterion and 3% from the depth of the maximum  
 176 temperature (here referred as other possibility). The threshold temperature criterion ( $0.2^\circ\text{C}$ )  
 177 gives the majority proportion with 54% of the MLD. In their study **Holte and Talley (2009)**  
 178 obtained 58% of the MLD with the « adjustment lines criterion », 22% with the threshold  
 179 criterion and 9% with the gradient criterion. The adjustment lines criterion using density  
 180 profiles determines the largest proportion of MLD corresponding to 49%, while 37% have been  
 181 estimated with the density threshold, 11% with the gradient criterion and 3% with the other  
 182 possibilities. These results show the importance of HT density algorithm in the determination  
 183 of the MLD with the density profiles and indicates the strong dependence of the MLD on the  
 184 structure of the density profile.

185 In addition, the MLD values determined from the other possibilities (3% on the temperature  
186 profiles and 3% on the density profiles) show that in the study area some salinity intrusions and  
187 temperature inversion occur and could lead to barrier layers. The results of this study are  
188 supported by **de Boyer Montégut et al. (2004)**, who identified and confirmed the existence of  
189 barrier layers in the western equatorial Pacific Ocean during all seasons (between 15° and 15°N  
190 and 150°E, 160°W), in all regions of the ITCZ (Intertropical Convergence Zone) and the South  
191 Pacific Convergence Zone, in the Bay of Bengal and the Eastern Equatorial Indian Ocean and  
192 in the western tropical Atlantic Ocean. In the tropical Atlantic Ocean, these barrier layers  
193 originate from advective processes or from the continental runoff of the Amazon River, as also  
194 concluded by **Sprintall and Tomczak (1992)**. The thick barrier layers of the western tropical  
195 Atlantic have also been detected in the deep tropical Atlantic basin, in the equatorial zone (5°S  
196 - 10°N) and could be associated in part with significant vertical temperature inversions (**Mignot  
197 et al., 2007**).

198 The results obtained from the study also confirm the existence of barrier layers in the eastern  
199 part of the Atlantic basin at 4°W as in the western tropical Atlantic. Indeed, according to the  
200 results of the HT algorithm, temperature inversions as well as salinity intrusions could be  
201 observed on the temperature and density profiles listed in Table 5 and represent 3% of the  
202 profiles on which the MLD were determined by the other possibilities.

203

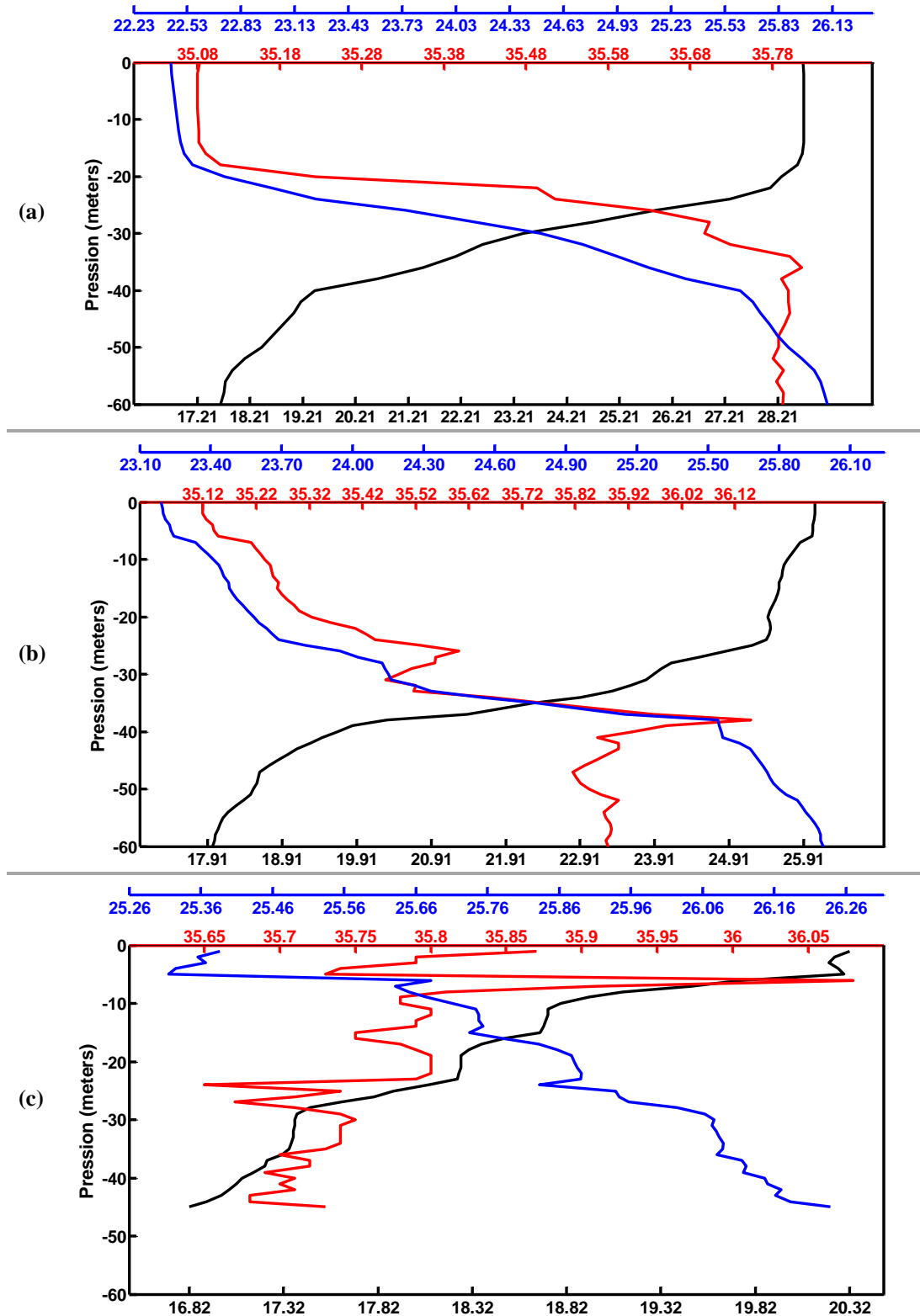
**Table 5:** Temperature and density profiles indicating salinity intrusions and temperature inversions and their MLD. Months indicate the numbers of corresponding months between 1 to 12. Stations 520 and 610 and their numbers are from SISMER. The other stations and their numbers are from WOD13. For abbreviations refer to Table 2

Temperature profiles					Density profiles				
Stations	Latitudes	Months	Years	MLD from temperature profiles (HT Temp Algo)	Stations	Latitudes	Months	Years	MLD from density profiles (HT Dens Algo)
3285750	4	5	1984	26	7744382	3	3	1993	29
7744382	3	3	1993	29	3374546	2,7483	3	1988	30
3374546	2,7	3	1988	30	3374546	2,7483	3	1988	30
3374546	2,7	3	1988	30	3287311	2	7	1984	29
3285744	2,5	5	1984	34	610	1,483	9	1978	30
3287311	2	7	1984	29	16025395	1,477	6	2014	36
610	1,5	9	1978	30	3321928	1,283	9	1972	32
16025395	1,5	6	2014	36	3332145	1	1	1977	26
3321928	1,3	9	1972	32	3322092	0,75	9	1972	30
3322092	0,8	9	1972	30	3336428	0,062	8	1978	26
520	0,6	8	1978	30	3336433	0,02	8	1978	32
3336428	0,1	8	1978	26					
3336433	0	8	1978	32					

204 **2.2. Analysis of visual determinations of MLD**

205 Visual inspections of profiles have been achieved for both coastal and equatorial zones for the  
 206 hot and cold season. These profiles have shown different hydrographic structures that can be  
 207 classified into three main types: The classical, the progressive and the graduated types as  
 208 suggested by **Tai et al. (2017)**. Examples of the three types of profiles encountered are shown  
 209 in Fig. 2.

210



211 **Fig. 2** Examples of different profiles types observed at 4°W. **Black line:** Temperature. **Red**  
 212 **line:** Salinity. **Blue line:** Density. **(a): Classical type:** MLD clearly identified by sudden  
 213 changes in depth gradients. Example: station 3374548; Year: 1988; Month: August;  
 214 Latitude: 4.2467°N. **(b): Progressive type:** MLD is not easily defined. Example: Example:  
 215 station: 3352851; Year: 1983; Month: October; Latitude: 4.8283°N. **(c): Graduated type:**  
 216 MLD not identified visually (profiles not considered). Example: station: 7728798; Year:  
 217 1998; Month: August; Latitude: 5.0107°N

218 The classical type structures show profiles with a surface layer without pronounced gradients,  
219 covering the main thermocline (or the pycnocline). The mixed layer is clearly differentiated by  
220 a sudden change in depth gradients. This classic type is the one that **Holte and Talley (2009)**  
221 call "summer profile".

222 Progressive type structures have slight temperature (or density) gradients in the mixed layer.  
223 The abrupt change in depth gradient that marks the boundary of the mixed layer is not clearly  
224 identifiable, so the MLD is not easily defined. This second type seems to be the one **Holte and**  
225 **Talley (2009)** call "winter profile".

226 Graduated type structures have successive pronounced gradients that do not allow easy  
227 identification and measurement of the MLD. Hence, the latter structures were not considered  
228 for the rest of the study. Of the two remaining profile types, the results indicate that 69% of  
229 MLD were determined on "summer profiles" and 31% on "winter profile".

230 Our results differ from those of **Tai et al. (2017)** who obtain about 85% of classical and  
231 progressive type profiles in their study of the structure of surface water and the thickness of the  
232 mixed layer in the tropical waters of the North China Sea over the period 1997-2013.

### 233 **2.3. Evaluation of methods using Taylor diagrams**

234 The Taylor diagrams between the numerical variants and their respective references to  
235 temperature and density profiles in hot and cold seasons are shown in Fig. 3. Table 6 presents  
236 the statistical parameters derived from these Taylor diagrams.

237

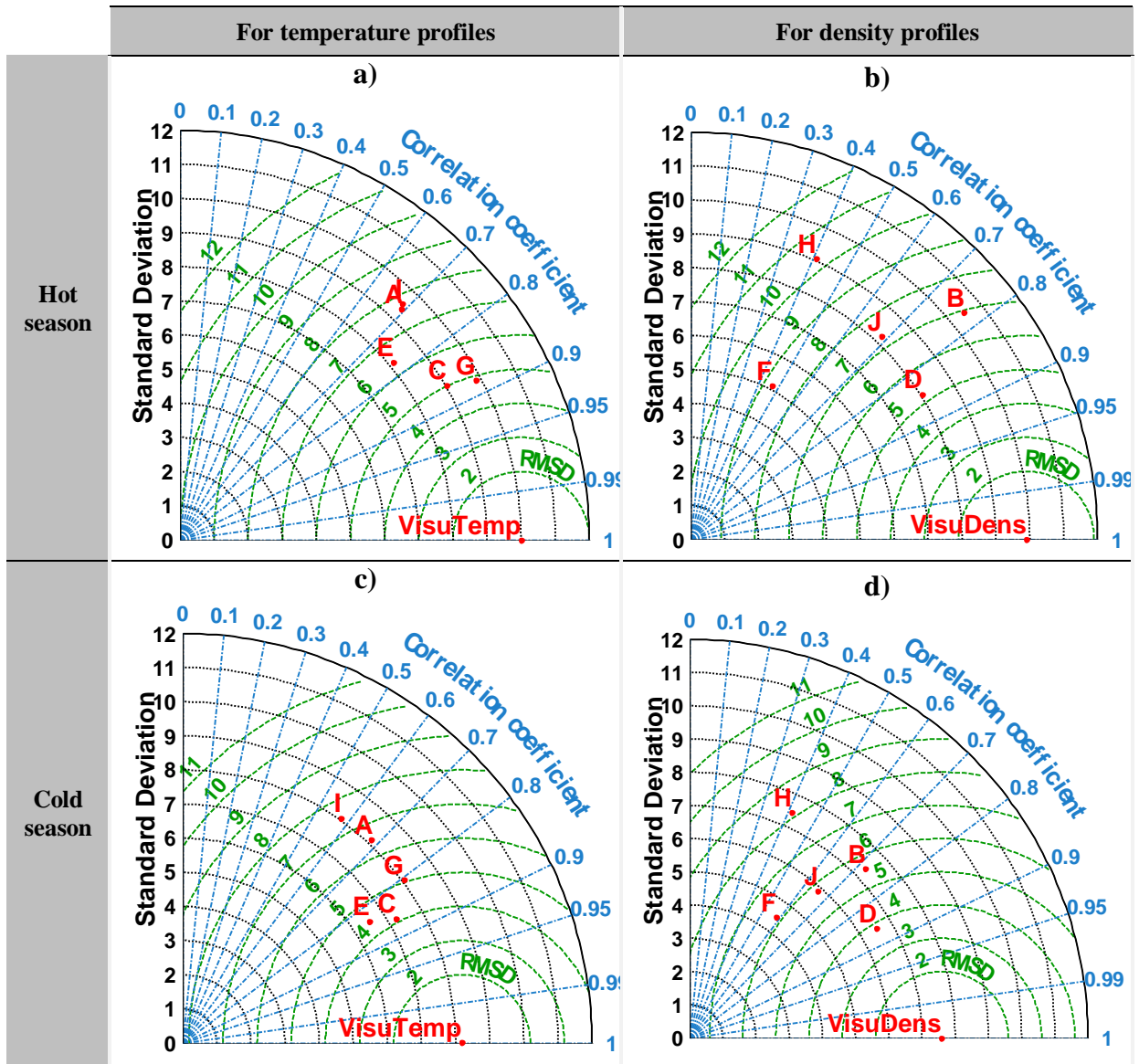


**Fig. 3** Taylor diagrams: Comparison between numerical methods and visual determinations during hot (a, b) and cold (c, d) season. A: HT Temp Algo, B: HT Dens Algo, C: HT Temp Thres, D: HT Dens Thres, E: HT Temp Grad, F: HT Dens Grad, G: LORB Temp, H: LORB Dens, I: TF Temp, J: TF Dens. RMSD: Root-Mean Square Deviation

238  
 239  
 240  
 241  
 242  
 243  
 244  
 245  
 246  
 247  
 248  
 249  
 250  
 251

**Table 6:** Statistical parameters from Taylor diagram based on the reference Visu Dens. The MLD estimates from variants B, D, F, H and J are compared to those from visual determination on density profiles. RMSD: Root-Mean-Square Deviation. r and R<sup>2</sup>: Bravais-Pearson correlation coefficient. For abbreviations refer to Table 2.

	Statistical parameters	Reference (Visu Dens)	HT Dens Algo (B)	HT Dens Thres (D)	HT Dens Grad (F)	LORB Dens (H)	TF Dens (J)
Hot season	Means	18,64	22,47	19,16	13,43	13,30	21,94
	Standard deviations	9,90	10,48	8,05	5,11	9,06	8,20
	RMSD	0	6,94	5,24	8,73	10,33	7,34
	r	1,00	0,77	0,85	0,47	0,41	0,69
Cold season	Means	17,09	20,46	18,90	13,30	14,38	19,62
	Standard deviations	7,60	7,34	6,53	4,49	7,45	5,87
	RMSD	0	5,59	3,84	6,17	8,15	5,78
	r	1,00	0,72	0,86	0,58	0,41	0,66

252 Three different statistics are analyzed: mean, standard deviation (STD), Root-Mean-Square  
 253 Deviation (RMSD) and the correlation coefficient of Bravais-Pearson (r instead of R<sup>2</sup>). The  
 254 lower the RMSD, the closer the variant is to the reference and is therefore able to reproduce the  
 255 reference values (**Taylor, 2001**).

256 The results show that, with the density profiles, the point representing the variant D (HT Dens  
 257 Thres) is closer to the reference (Visu Dens) than all the other points in the hot season and in  
 258 the cold season. Statistics from Taylor diagrams indicate that only the two variants, B (HT Dens  
 259 Algo) and D (HT Dens Thres) have high correlation coefficients. HT Dens Thres is nevertheless  
 260 the highest compared to the other variants (B, J, F, H) and is 0.85 in hot season and 0.86 in cold  
 261 season. Its standard deviation is 8.05 during the hot season and 6.53 during the cold season, and  
 262 its distance from Visu Dens (RSMD) is 5.24 and 3.84, respectively, in hot and cold seasons. In  
 263 addition, the average MLD determined with HT Dens Thres are the closest to the MLD averages  
 264 visually determined on the density profiles.

265 The Taylor diagrams based on the Visu Temp reference show that three variants, C (HT Temp  
 266 Thres), E (HT Temp Grad) and G (LORB Temp) are the closest to the reference with respect to  
 267 two other variants A and I (Fig. 3). In addition, Table 7 shows the statistical parameters  
 268 determined for these diagrams based on the temperature profiles.

269

270

271

**Table 7:** Statistical parameters from Taylor diagram based on the reference Visu Temp. The MLD estimates from variants A, C, E, G and I are compared to those from visual determination on temperature profiles. RMSD: Root-Mean-Square Deviation.  $r$  and  $R^2$ : Bravais-Pearson correlation coefficient. For abbreviations refer to Table 2.

	Statistical parameters	Reference: Visu Temp	HT Temp Algo (A)	HT Temp Thres (C)	HT Temp Grad (E)	LORB Temp (G)	TF Temp (I)
Hot season	Means	19,42	25,08	23,76	17,71	19,64	25,32
	Standard deviations	10,00	9,36	9,03	8,14	9,86	9,51
	RMSD	0	7,61	5,01	6,40	4,86	7,74
	$r$	1,00	0,69	0,87	0,77	0,88	0,69
Cold season	Means	17,35	21,86	20,79	16,53	18,24	21,23
	Standard deviations	8,19	8,12	7,23	6,53	8,07	8,05
	RMSD	0	6,51	4,11	4,46	5,08	7,47
	$r$	1,00	0,68	0,87	0,84	0,80	0,58

272 The same variants HT Temp Thres, HT Temp Grad and LORB Temp have the strongest  
 273 correlations with Visu Temp unlike TF Temp for both seasons. However, the RMSD values of  
 274 variants HT Temp Thres and LORB Temp are the weakest. For variant LORB Temp in hot  
 275 season (RMSD = 4.86, mean = 19.64 against 19.42 for reference) and for HT Temp Thres in  
 276 cold season (RMSD = 4.11, mean = 20.79 against 17.35 for the reference).

277 The different results seem to show that, whatever the season, the HT Dens Thres variant of the  
 278 HT method is the most appropriate for determining the MLD from the density profiles. With  
 279 the temperature profiles the results of the Taylor diagrams show at this stage that are the variants  
 280 LORB Temp and HT Temp Thres that should be used to determine the MLD respectively in  
 281 hot season and cold season. Since it is impossible to definitively conclude from the Taylor  
 282 diagrams at least as regards the temperature profiles, it is necessary to observe the 2D diagrams  
 283 to refine the choice of the appropriate method.

#### 284 **2.4. Evaluation of methods using correlation diagrams**

285 The  $p$ -values and linear correlation coefficients between the numerical methods HT, LORB, TF  
 286 and the visual methods are given in Table 8.

287

288

289

290

291

**Table 8:** *p-value* and correlation coefficients between numerical and visual estimates for hot and cold season. Correlation coefficients substantially greater than 0.519 are in bold. For abbreviations refer to Table 2.

	Methods variants	<i>p-values</i>		Correlation coefficients (R <sup>2</sup> )	
		Visu Temp	Visu Dens	Visu Temp	Visu Dens
Hot season	HT Temp Algo	5.63.E-38	3.86.E-33	0.48036	0.432977
	HT Dens Algo	7.07.E-47	1.92.E-51	<b>0.557546</b>	<b>0.592607</b>
	HT Temp Thres	1.38.E-78	1.69.E-68	<b>0.750718</b>	<b>0.70077</b>
	HT Dens Thres	1.07.E-67	1.92.E-72	<b>0.696407</b>	<b>0.721395</b>
	HT Temp Grad	2.32.E-51	8.29.E-50	<b>0.591992</b>	<b>0.580385</b>
	HT Dens Grad	7.61.E-16	1.13.E-15	0.226072	0.223701
	LORB Temp	2.48.E-84	1.47.E-83	<b>0.775351</b>	<b>0.772184</b>
	LORB Dens	7.03.E-12	1.02.E-11	0.169291	0.166889
	TF Temp	5.51.E-37	2.81.E-33	0.470994	0.434373
	TF Dens	7.03.E-34	5.85.E-37	0.440484	0.470733
Cold season	HT Temp Algo	7.9.E-37	8.3.E-29	0.464238	0.382221
	HT Dens Algo	2.48.E-39	5.94.E-43	0.487553	<b>0.519509</b>
	HT Temp Thres	2.7.E-79	3.45.E-58	<b>0.748485</b>	<b>0.633648</b>
	HT Dens Thres	1.58.E-68	1.19.E-78	<b>0.695272</b>	<b>0.74558</b>
	HT Temp Grad	2.67.E-70	4.19.E-51	<b>0.704743</b>	<b>0.584384</b>
	HT Dens Grad	2.02.E-27	4.E-25	0.366836	0.340542
	LORB Temp	1.95.E-60	5.07.E-45	<b>0.648025</b>	<b>0.536879</b>
	LORB Dens	2.84.E-13	3.57.E-12	0.187022	0.171173
	TF Temp	1.79.E-24	5.22.E-19	0.332883	0.265174
	TF Dens	8.14.E-33	6.92.E-34	0.424648	0.435481

292 The 2D correlation diagrams between these variants and the Visu Temp and Visu Dens  
293 references in hot and cold seasons are shown in Fig. 4 and 5. All the *p-value* are < 0.05,  
294 indicating that all correlations are highly significant at the 5% level. The analysis of the values  
295 of the correlation coefficients shows that five variants have stronger correlations with Visu  
296 Temp and Visu Dens references in hot and cold seasons. These are HT Dens Algo and HT Dens  
297 Thres on density profiles, HT Temp Thres, HT Temp Grad and LORB Temp on temperature  
298 profiles.

299

300

301

302

303

304

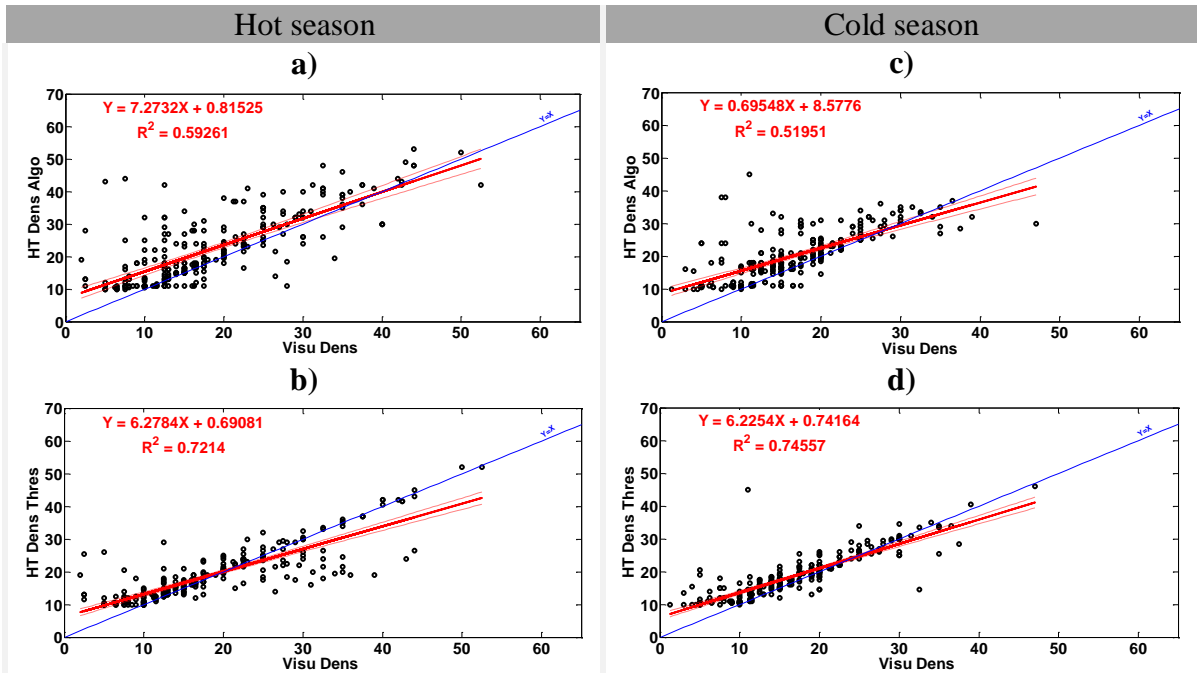


**Fig. 4** 2D correlation diagrams between Visu Dens and both variants B (HT Dens Algo) and D (HT Dens Thres) for MLD estimated from density profiles. Diagrams a, b for hot season and c, d for cold season.

305

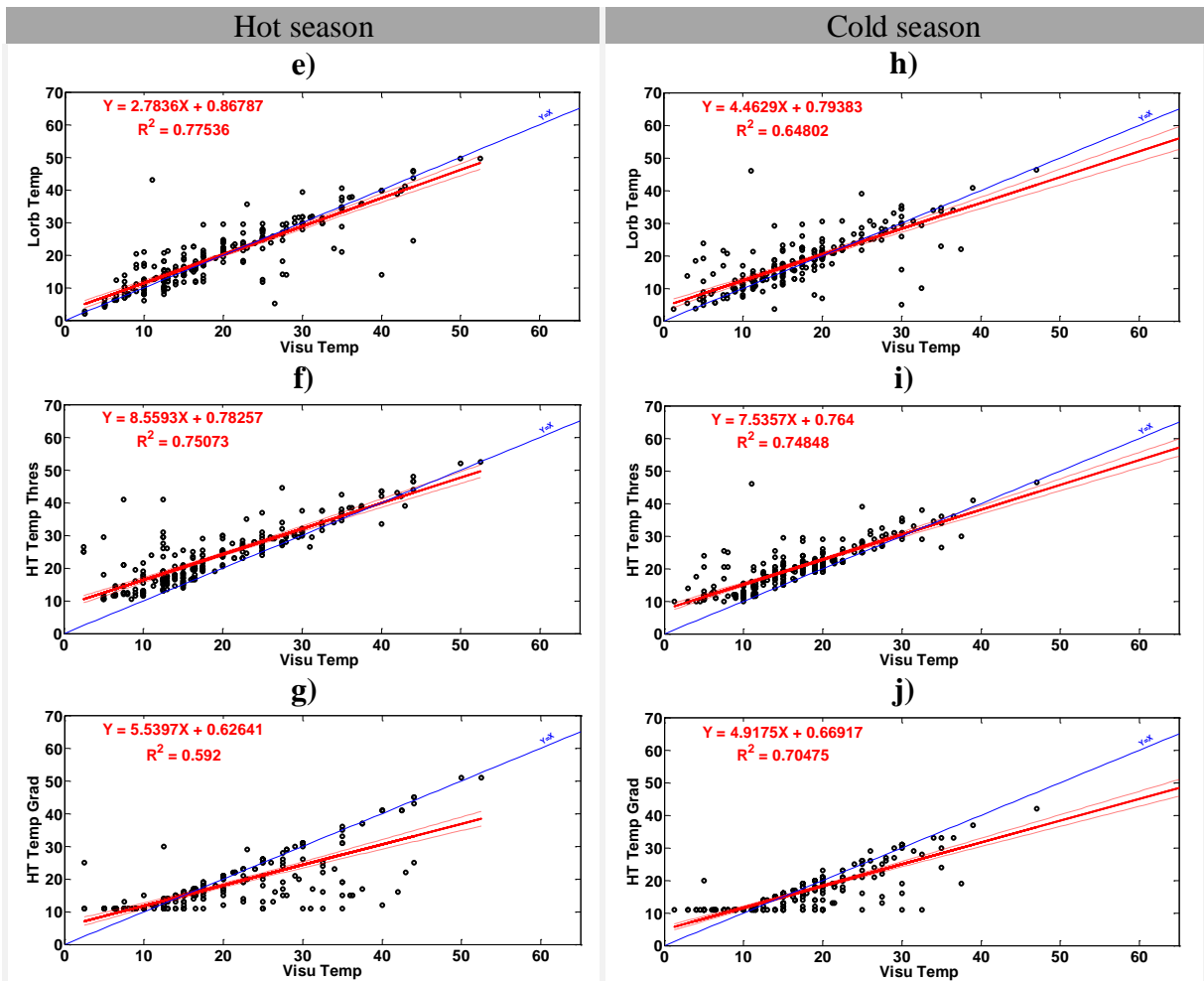


**Fig. 5** 2D correlation diagrams between Visu Temp and the three variants C (HT Temp Thres), E (HT Temp Grad) and G (LORB Temp) for MLD estimated from temperature profiles. Hot season (e, f, g). Cold season (h, i, j).

306 With the temperature profiles, the 2D diagrams show that HT Temp Thres overestimates the  
307 MLD, HT Temp Grad underestimates them, while LORB Temp gives MLD comparable to the  
308 Visu Temp reference.

309 Our results show that the de Boyer Montegut density threshold method (potential density) with  
310 the constant criterion  $\Delta\sigma = 0.03 \text{ kg.m}^{-3}$  and a reference depth of ten meters is the most  
311 appropriate for determining the MLD in the Gulf of Guinea regardless the season. These results  
312 thus point to the prevalence of the threshold criterion and the choice of density (which takes  
313 into account both temperature and salinity) in the determination of the MLD. **Schneider and**  
314 **Müller (1990)**, **Brainerd and Gregg (1995)** as well as **Thomson and Fine (2003)**  
315 demonstrated that the MLD obtained from a threshold criterion is more stable than the MLD  
316 based on a gradient criterion and give values that are closer to the "real" MLD. Moreover,  
317 according to **Lukas and Lindstrom (1991)**, a criterion based on potential density produces  
318 more reliable MLD than a temperature criterion because the temperature would not adequately  
319 account for vertical stratification in many regions. This is corroborated by **Thomson and Fine**  
320 **(2003)** who recommend using the potential density for the MLD because the density directly  
321 affects the stability and degree of turbulent mixing of the water column. In addition, the  
322 existence of barrier layers, as shown by our results, generally leads to the definition of the depth  
323 of the mixing layer more adequately by a density criterion (**Peter, 2007**).

324 In the situation where temperature profiles data are only available it is advisable to estimate  
325 MLD using the **Lorbacher** curvative method. The MLD determined with the temperature  
326 profiles overestimate those obtained with the density profiles whatever the chosen criterion  
327 (threshold, gradient, alternative algorithms). In particular, the method based on the temperature  
328 threshold  $\Delta T = 0.2^\circ\text{C}$  of **de Boyer Montegut et al. (2004)** overestimates the MLD compared  
329 to the method of **Lorbacher et al. (2006)** applied to temperatures. These results are in  
330 agreement with those of **Lukas and Lindstrom (1991)** and **Sprintall and Tomczak (1992)**  
331 who have shown that threshold methods, especially those based solely on temperature,  
332 intrinsically overestimate MLD. To support this result, **Holte and Talley (2009)**, whose work  
333 has addressed the Sub-Antarctic Water Formation and Antarctic Intermediate Water regions,  
334 also found that threshold methods tend to overestimate the MLD compared to temperature and  
335 density algorithms.

336

337

338 **CONCLUSION**

339 Five hundred and sixteen (516) MLD values including 260 for the cold season and 256 for the  
340 hot season are determined using the HT, TF and LORB numerical methods. The maximum  
341 MLD are obtained from the temperature profiles with the TF and HT methods and the lowest  
342 MLD with LORB methods regardless the season. These numerical results, compared with the  
343 visual measurements (representing the reference values obtained by visual inspection of all the  
344 516 profiles of temperature and density) through statistical and graphical analyses using the  
345 Taylor and 2D correlation diagrams, show that the HT density threshold method (potential  
346 density) with the constant criterion  $\Delta\sigma = 0.03 \text{ kg.m}^{-3}$  and a reference depth of ten meters is the  
347 most appropriate for determining the MLD in the Gulf of Guinea regardless the season. In the  
348 situation where temperature profiles data are only available it is advisable to estimate MLD  
349 using the Lorbacher curvative method.

350

351 **Conflict of Interest statement:** On behalf of all authors, the corresponding author states that  
352 there is no conflict of interest.

- Alboukadel K (2018)** ggcorrplot: Visualization of a Correlation Matrix using 'ggplot2'. R package version 0.1.2. <https://CRAN.R-project.org/package=ggcorrplot>
- Binet D, Marchal E (1993)** The Large Marine Ecosystem of Shelf Areas in the Gulf of Guinea: Long-Term Variability Induced by Climatic Changes. In: Large Marine Ecosystems - Stress Mitigation and Sustainability. K. Sherman, L.M. Alexander and B. Gold, Eds. American Association for the Advancement of Science, Washington. pp. 104-118.
- Boyer TP, Antonov JI, Baranova OK, Coleman C, Garcia HE, Grodsky A, Johnson DR, Locarnini RA, Mishonov AV, O'Brien TD, Paver CR, Reagan JR, Seidov D, Smolyar IV, Zweng MM (2013)** World Ocean Database 2013. Sydney Levitus, Ed.; Alexey Mishonov, Technical Ed.; NOAA Atlas NESDIS 72, 209 pp.
- Brainerd KE, Gregg MC (1995)** Surface mixed and mixing layer depths, Deep Sea Res., Part I, 42(9), 1521–1543.
- de Boyer Montégut C, Madec G, Fischer AS, Lazar A, Ludicone D (2004)** Mixed layer depth over the global ocean: an examination of profile data and a profile-based climatology. Journal of Geophysical Research, 109:C12003. doi : 10.1029/2004JC002378.
- Hardman-Mountford NJ (2000)** Environmental variability in the Gulf of Guinea large marine ecosystem: physical features, forcing and fisheries. PhD thesis, University of Warwick.
- Holte J, Talley L (2009)** A New Algorithm for Finding Mixed Layer Depths with Applications to Argo Data and Subantarctic Mode Water Formation. J. Atmos. Oceanic Technol., 26, 1920–1939, <https://doi.org/10.1175/2009JTECHO543.1>
- Kara AB, Rochford PA, Hurlburt HE (2000)** An optimal definition for ocean mixed layer depth. Journal of Geophysical Research., 105(C7), 16,803–16,821. <https://doi.org/10.1029/2000JC900072>
- Kara AB, Rochford PA, Hurlburt HE (2003)** Mixed layer depth variability over the global ocean. J Geophys Res. 108: 1–15. doi: 10.1029/2000JC000736
- Lorbacher K, Dommenges D, Niiler PP, Köhl A (2006) Ocean mixed layer depth. A subsurface proxy of ocean-atmosphere variability, J. Geophys. Res.-Oceans, 111, 1–22, <https://doi.org/10.1029/2003JC002157>, 2006.
- Lukas R, Lindstrom E (1991)** The mixed layer of the western equatorial Pacific Ocean, J. Geophys. Res., 96(S01), 3343–3357, doi:10.1029/90JC01951.
- Maheswaran PA (2004)** Mixed Layer Characteristics and Hydrography off the West and East Coasts of India. Cochin University of Science and Technology. Fac. Mar. Sci. Kerala, India. <http://dyuthi.cusat.ac.in/purl/779>
- Mignot J, de Boyer Montégut C, Lazar A, Cravatte S (2007)** Control of salinity on the mixed layer depth in the world ocean: 2. Tropical areas, J. Geophys. Res., 112, C10010, doi:10.1029/2006JC003954.
- Nahavandian ES (2014)** Temporal and spatial evolution of the mixed layer in the southern Beaufort Sea and the Amundsen Gulf. Thèse. Québec, Université du Québec, Institut national de la recherche scientifique, Doctorat en sciences de l'eau, 223 p
- Nieto K, Mélin F (2017)** Variability of chlorophyll-a concentration in the Gulf of Guinea and its relation to physical oceanographic variables. Prog. Oceanogr., 151, pp. 97-115. <https://doi.org/10.1016/j.pocean.2016.11.009>
- Ohno Y, Iwasaka N, Kobashi F et al. (2009)** Mixed layer depth climatology of the North Pacific based on Argo observations. J Oceanogr 65: 1. <https://doi.org/10.1007/s10872-009-0001-4>
- Peter AC, Le Hénaff M, du Penhoat Y, Menkès C E, Marin F et al. (2006)** A model study of the seasonal mixed layer heat budget in the equatorial Atlantic. Journal of Geophysical Research, American Geophysical Union. 111, pp.C06014. doi: 10.1029/2005JC003157

- Peter AC (2007)** Variabilité de la température de la couche de mélange océanique en Atlantique équatorial aux échelles saisonnières à interannuelles, à l'aide de simulation numérique. Océan, Atmosphère. Université Paul Sabatier – Toulouse III. French. <tel-00157983>
- Schneider N, Müller P (1990)** The meridional and seasonal structure of the mixed-layer depth and its diurnal amplitude observed during the Hawaii-to-Tahiti Shuttle experiment. *Journal of Physical Oceanography*, 20(9):1395-1404
- Sprintall J, Roemmich D (1999)** Characterizing the structure of the surface layer in the Pacific ocean. *J. Geophys. Res.*, 104(C10):23297-23311. <https://doi.org/10.1029/1999JC900179>
- Sprintall J, Tomczak M (1992)** Evidence of the barrier layer in the surface layer of the tropics. *J. Geophys. Res.*, 97, 7305–7316. <https://doi.org/10.1029/92JC00407>
- Tai JH, Wong GTF, Pan X (2017)** Upper water structure and mixed layer depth in tropical waters: The SEATS station in the northern South China Sea. *Terr. Atmos. Ocean. Sci.*, 28, 1019-1032, doi: 10.3319/TAO.2017.01.09.01
- Tanguy Y, Arnault S, Philippe L (2010)** Isothermal, mixed, and barrier layers in the subtropical and tropical Atlantic Ocean during the ARAMIS experiment. *Deep Sea Research Part I: Oceanographic Research Papers*. 57. 501-517. 10.1016/j.dsr.2009.12.012.
- Taylor KE (2001)** Summarizing multiple aspects of model performance in a single diagram. *J. Geophys. Res.* 106: 7183–7192. doi:10.1029/2000JD900719.
- Thomson RE, Fine IV (2003)** Estimating Mixed Layer Depth from Oceanic Profile Data. *J. Atmos. Oceanic Technol.*, 20, 319-329. [https://doi.org/10.1175/1520-0426\(2003\)020<0319:EMLDFO>2.0.CO;2](https://doi.org/10.1175/1520-0426(2003)020<0319:EMLDFO>2.0.CO;2)
- Thomson RE, Fine IV (2009)** A Diagnostic Model for Mixed Layer Depth Estimation with Application to Ocean Station P in the Northeast Pacific. *J. Phys. Oceanogr.*, 39, 1399–1415, <https://doi.org/10.1175/2008JPO3984.1>
- Tilot V, King A (1993)** A review of the subsystems of the canary current and Gulf of Guinea large marine ecosystems. IUCN Marine Programme. *In* Hardman-Mountford NJ (2000) Environmental variability in the Gulf of Guinea large marine ecosystem: physical features, forcing and fisheries. PhD thesis, University of Warwick
- Wade M (2010)** Caractérisation de la couche limite océanique pendant les campagnes EGEE/AMMA dans l'Atlantique Équatorial Est. Océan, Atmosphère. Université Paul Sabatier - Toulouse III. <tel-01020065>
- You Y (1995)** Salinity Variability and Its Role in the Barrier-Layer Formation during TOGA-COARE. *J. Phys. Oceanogr.*, 25, 2778–2807, [https://doi.org/10.1175/1520-0485\(1995\)025<2778:SVAIRI>2.0.CO;2](https://doi.org/10.1175/1520-0485(1995)025<2778:SVAIRI>2.0.CO;2)